Synthesis, Reactivity, and Structure of Strictly Homologous 18 and 19 Valence Electron Iron Nitrosyl Complexes**

Dieter Sellmann,*[a] Nicole Blum,[a] Frank W. Heinemann,[a] and Bernd A. Hess*[b]

Abstract: The 18 and 19 valence electron (VE) nitrosyl complexes [Fe(NO)($'pyS_4'$)]BF_4 ([**1**]BF_4) and [Fe(NO)($'pyS_4'$)] (**2**) have been synthesized from [Fe($'pyS_4'$)]$_x$ ($'pyS_4{}^{2-}$ = 2,6-bis(2-mercaptophenylthiomethyl)pyridine(2−)) and either $NOBF_4$ or NO gas. Complex [**1**]BF_4 was also obtained from [Fe(CO)($'pyS_4'$)] and $NOBF_4$. The cation [**1**]$^+$ is reversibly reduced to give **2**. Oxidation of **2** by [Cp_2Fe]PF_6 afforded [Fe(NO)($'pyS_4'$)]PF_6 ([**1**]PF_6). The molecular structures of [**1**]PF_6 and **2** were determined by X-ray crystallography. They demonstrate that addition of one electron to [**1**]$^+$ causes a significant elongation of the Fe-donor atom bonds and a bending of the FeNO angle. Density functional calculations show that the unpaired electron in **2** occupies an orbital, which is antibonding with respect to all Fe-ligand interactions. As expected from qualitative Molecular Orbital (MO) theory, it has a large contribution from a π* type NO orbital. The ν(NO) frequency decreases from 1893 cm^{-1} in [**1**]BF_4 to 1648 cm^{-1} in **2** (in KBr). The antibonding character of the unpaired electron explains the ready reaction of **2** with excess NO to give [Fe(NO)$_2$($'pyS_4'$)] (**3**), the facile NO/CO exchange of **2** to afford [Fe(CO)($'pyS_4'$)], and the easy oxidation of **2** to [**1**]$^+$.

Keywords: density functional calculations · iron · nitrosyl complexes · S ligands · structure elucidation

Introduction

The specific electronic, structural, and reactivity features of transition metal nitrosyl complexes have aroused interest since the early days of coordination chemistry. More recent is the interest in nitrosyl complexes as potential waste gas purification catalysts,[1] as drugs that release the neurotransmitter and mammalian bioregulator NO,[2] or as model complexes for metal enzymes such as the nitrile hydratase,[3] cytochrome oxidase,[4] and nitrogenases.[5] For example, NO strongly inhibits N_2 fixation[5] and in a few cases, NO complexes served as precursors for N_2 complexes,[6] which are taken to represent the primary species when N_2 binds to the active sites of FeMo, FeV, or FeFe nitrogenases.[5]

Most nitrosyl complexes are 18 valence electron (VE) complexes.[6b, 7] In a very few cases, such complexes could be reduced to give 19 VE species.[7, 8] In this context a fundamental question with regard to the electronic structure and reactivity of 19 VE nitrosyl complexes is the character of the orbital populated by the single electron. For the few accessible and investigated 19 VE nitrosyl complexes, the discussion ranges from NO-centered to metal-centered and to coligand-centered orbitals.[7–9]

To the best of our knowledge and despite the long history of nitrosyl complexes a couple of structurally characterized homologous 18 and 19 VE nitrosyl complexes have never been described. However a true understanding of the electronic situation is only possible when the correct molecular structures of the discussed species are known.

Here we want to describe the evidently first couple of 18 and 19 VE nitrosyl complexes that have strictly identical donor atom sets as well as atom connectivities, and could be characterized by X-ray structure analysis. These complexes are part of the results obtained in attempts to synthesize nitrosyl complexes of the [Fe($'pyS_4'$)] fragment as precursor compounds for N_2 complexes. The [Fe($'pyS_4'$)] fragment contains the recently described pentadentate ligand 2,6-bis(2-mercaptophenylthiomethyl)pyridine(2−) ($'pyS_4{}^{2-}$).[10] Its bismethylene pyridine unit enforces the *trans* coordination of the thiolate donors as indicated by formula A.

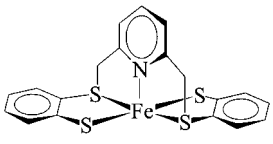

[a] Prof. Dr. D. Sellmann, Dipl.-Chem. N. Blum, Dr. F. W. Heinemann
Institut für Anorganische Chemie
der Universität Erlangen-Nürnberg
Egerlandstrasse 1, 91058 Erlangen (Germany)
Fax: (+49) 9131-8527367
E-mail: sellmann@anorganik.chemie.uni-erlangen.de

[b] Prof. Dr. B. A. Hess
Institut für Physikalische und Theoretische Chemie
der Universität Erlangen-Nürnberg
Egerlandstrasse 3, 91058 Erlangen (Germany)
Fax: (+49) 9131-8527736
E-mail: hess@chemie.uni-erlangen.de

[**] Transition Metal Complexes with Sulfur Ligands, Part 147; for Part 146 see: D. Sellmann, F. Geipel, F. W. Heinemann, *Chem. Eur. J.* **2000**, *6*, 4279–4284.

0947-6539/01/0709-1874 $ 17.50+.50/0

Results and Discussion

Syntheses and reactions of [Fe(L)(′pyS$_4$′)] complexes: Scheme 1 summarizes the syntheses and reactions of [Fe(L)(′pyS$_4$′)] complexes. The first target complex was [Fe(NO)(′pyS$_4$′)]BF$_4$ ([**1**]BF$_4$). In a straightforward reaction, light

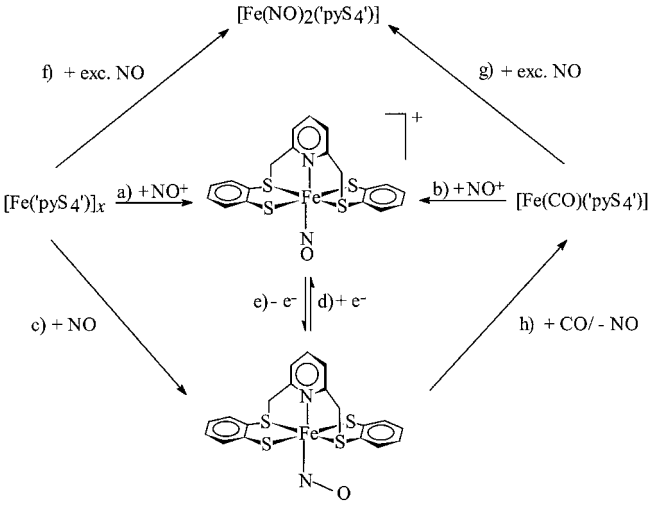

Scheme 1. Syntheses and reactions of [Fe(L)(′pyS$_4$′)] complexes: a) CH_2Cl_2, $NOBF_4$, 25 °C; b) CH_2Cl_2, $NOBF_4$, 0 °C; c) CH_2Cl_2, 1 equiv of NO (g), 25 °C; d) CH_2Cl_2, N_2H_4, NH_3, $NaNH_2$, NEt_4N_3, $BuNH_2$, MeOH, or DMF, 25 °C; e) CH_2Cl_2, $[Cp_2Fe]PF_6$, −78 °C; f) CH_2Cl_2, excess NO (g), 25 °C; g) CH_2Cl_2, excess NO (g), 25 °C; h) CH_2Cl_2, excess NO (g), 25 °C.

brown [**1**]BF$_4$ formed when a suspension of the parent complex [Fe(′pyS$_4$′)]$_x$ in CH_2Cl_2 was treated with one molar equivalent of $NOBF_4$ (Scheme 1, reaction a). The solid-state structure of [Fe(′pyS$_4$′)]$_x$ could not be determined yet, however, x is probably 2.[10, 11] The formation of [**1**]BF$_4$ could be monitored by its ν(NO) IR band at 1901 cm^{-1} in CH_2Cl_2. Complex [**1**]BF$_4$ also formed when a solution of [Fe(CO)(′pyS$_4$′)] in CH_2Cl_2 was treated with $NOBF_4$ at 0 °C according to reaction b. This procedure, however, required more purification steps and gave lower yields of [**1**]BF$_4$.

Treatment of [Fe(′pyS$_4$′)]$_x$ with one molar equivalent of NO gas gave the neutral 19 VE complex [Fe(NO)(′pyS$_4$′)] (**2**), which exhibits a ν(NO) IR band at 1670 cm^{-1} in CH_2Cl_2 (Scheme 1, reaction c). In this synthesis, the use of the exact stoichiometric amount of NO proved to be essential in order to avoid the formation of by-products such as [Fe(NO)$_2$(′pyS$_4$′)] (**3**) (see below).

Complexes [**1**]BF$_4$ and **2** are soluble in CH_2Cl_2, acetone, or DMF. The 19 VE complex **2** is paramagnetic. Its magnetic moment of $\mu_{eff} = 1.71\ \mu_B$ (293 K) corresponds to one unpaired electron. Diamagnetic [**1**]BF$_4$ exhibits a ^{1}H NMR spectrum which is typical for the [M(′pyS$_4$′)] fragment,[10–12] which shows the benzene and the pyridine proton signals in the range of $\delta = 7.80 - 7.20$ and two doublets for the methylene CH_2 groups at $\delta = 5.56$ and $\delta = 4.95$. The ^{13}C NMR spectrum shows one signal for the methylene groups at $\delta = 51.6$ and only nine aromatic signals between $\delta = 156.3$ and 122.8. The number of ten signals in total in the ^{13}C NMR spectrum indicates C_2 symmetry of [**1**]$^+$ in solution.

The mass spectra of both [**1**]BF$_4$ and **2** exhibit relatively weak peaks for the [Fe(NO)(′pyS$_4$′)]$^+$ cation at $m/z = 471$ and strong peaks for the fragment ion [Fe(′pyS$_4$′)]$^+$ and the dimer [Fe(′pyS$_4$′)]$_2^+$ at $m/z = 441$ and 882; these spectra indicate a ready NO dissociation as well as dimerization of [Fe(′pyS$_4$′)] fragments.

The cyclic voltammograms (CV) of [**1**]BF$_4$ and **2** are identical. Figure 1 exemplarily shows the CV of **2** in DMF. The reversible redox wave in the anodic region at $E_{1/2} = 0.11$ V can

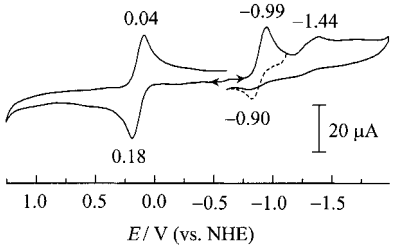

Figure 1. Cyclic voltammogram of [Fe(NO)(′pyS$_4$′)] in DMF ($\nu = 100$ mV s^{-1}).

be assigned to the redox couple [Fe(NO)(′pyS$_4$′)]$^{0/+}$. The redox wave in the cathodic region at $E_{1/2} = -0.99$ V becomes reversible upon increasing the scan rate to 500 mV s^{-1} and reversing the current at −1.23 V. The resulting redox wave at $E_{1/2} = -0.95$ V indicates that the 19 VE complex **2** can be reduced further to give [Fe(NO)(′pyS$_4$′)]$^-$. This species may be considered as a 20 VE complex or as an 18 VE complex, in which a two-electron NO$^-$ ligand binds to a 16 VE [Fe(′pyS$_4$′)] fragment. The [Fe(NO)(′pyS$_4$′)]$^-$ species evidently is very labile. Its decomposition products might give rise to the irreversible redox wave at −1.44 V.

The redox interconversion of [**1**]BF$_4$ and **2** was also achieved chemically. Complex [**1**]BF$_4$ was readily reduced by hydrazine to give **2** (Scheme 1, reaction d). Vice versa, $[Cp_2Fe]PF_6$ oxidized **2** to afford [Fe(NO)(′pyS$_4$′)]PF$_6$ ([**1**]PF$_6$) according to reaction e. The formation of [**1**]PF$_6$ could be monitored by solution IR spectroscopy, which showed the decrease of the ν(NO) band of **2** at 1670 cm^{-1} and the simultaneous increase of the ν(NO) band of [**1**]PF$_6$ at 1902 cm^{-1} (Figure 2).

The complex salts [**1**]PF$_6$ and [**1**]BF$_4$ have practically identical properties. Complex [**1**]PF$_6$ could be obtained in single crystalline form, which enabled the X-ray structural characterization and comparison of the cation [**1**]$^+$ with its neutral counterpart **2** (see below).

The high ν(NO) frequency of [**1**]BF$_4$ (1901 cm^{-1} in CH_2Cl_2, 1893 cm^{-1} in KBr) made the [**1**]$^+$ cation a candidate for attempts to convert the NO into a N_2 ligand by addition of nitrogen nucleophiles to the nitrosyl N atom.[6b, c] For this purpose, [**1**]BF$_4$ was treated with NH_3, $NaNH_2$, or NEt_4N_3. However, in none of these cases did a nucleophilic addition to the NO ligand take place, and the nucleophiles acted rather as reductants yielding **2**. Subsequent experiments revealed that even nBuNH$_2$ or solvents such as MeOH or DMF could reduce the cationic [**1**]$^+$ to give neutral **2**.

Monitoring the reactions of [**1**]BF$_4$ with NH_3, $NaNH_2$, NEt_4N_3, or MeOH by IR spectroscopy showed that in

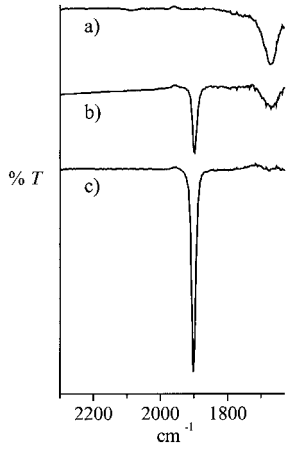

Figure 2. IR spectroscopic monitoring in CH_2Cl_2 of a) [Fe(NO)($'pyS_4'$)], b) 1 min, and c) 20 min after addition of $[Cp_2Fe]PF_6$.

addition to **2** another nitrosyl species formed exhibiting two ν(NO) bands of equal intensity at 1785 and 1755 cm^{-1} in CH_2Cl_2. The identical species formed as the main product in syntheses in which [Fe($'pyS_4'$)]$_x$ or [Fe(CO)($'pyS_4'$)] were treated with an excess of NO gas (Scheme 1, reactions f and g). A brown, sparingly soluble product formed whose elemental analysis and spectroscopic data were compatible with those for [Fe(NO)$_2$($'pyS_4'$)] (**3**). As judged from its ^{1}H NMR spectrum, **3** is diamagnetic and possesses C_1 symmetry. The formation of **3** can be rationalized by the lability of the 19 VE complex **2**, which is the primary product in the reaction between [Fe($'pyS_4'$)]$_x$ and NO (Scheme 1, reaction c). The lability of **2** may cause dissociation of one or more iron ligand donor bonds, and the dissociation gives rise to coordinatively unsaturated 17 or 15 VE species. The 15 VE species can be saturated by addition of a second NO molecule, for example, according to Scheme 2.

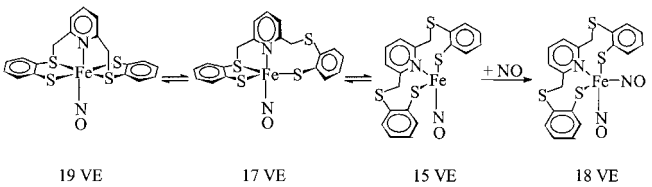

Scheme 2. Equilibria between 19, 17, 15, and 18 VE complexes. Saturation of the 15 VE species by addition of a second NO molecule.

Proof of such bond dissociation reactions was obtained when **2** was treated with an excess of CO gas at standard conditions (Scheme 1, reaction h). A rapid and complete NO/CO exchange took place, and the reaction yielded [Fe(CO)($'pyS_4'$)], which was identified by its ν(CO) IR band at 1976 cm^{-1} in CH_2Cl_2. This reaction is one of the very rare examples of substituting NO by CO. Usually, only the reverse exchange of CO for NO is possible.[13] A precedent for a NO/CO exchange was found with [Fe(NO)($'tBuS_5'$)], which is closely related to **2** ($'tBuS_5'^{2-}$ = 2,2′-bis(2-mercapto-3,5-di-*tert*-butylphenylthio)-diethylsulfide(2 –)).[14]

X-ray structure determination of [Fe(NO)($'pyS_4'$)]PF_6 ([1]PF_6) and [Fe(NO)($'pyS_4'$)]·2CH_2Cl_2 (2·2CH_2Cl_2): Complexes [**1**]PF_6 and **2** yielded single crystals upon recrystallization. Complex **2** was obtained as the solvate **2**·2CH_2Cl_2. The X-ray structure determinations showed that both compounds contain discrete cations, anions, or molecules. Figure 3 depicts

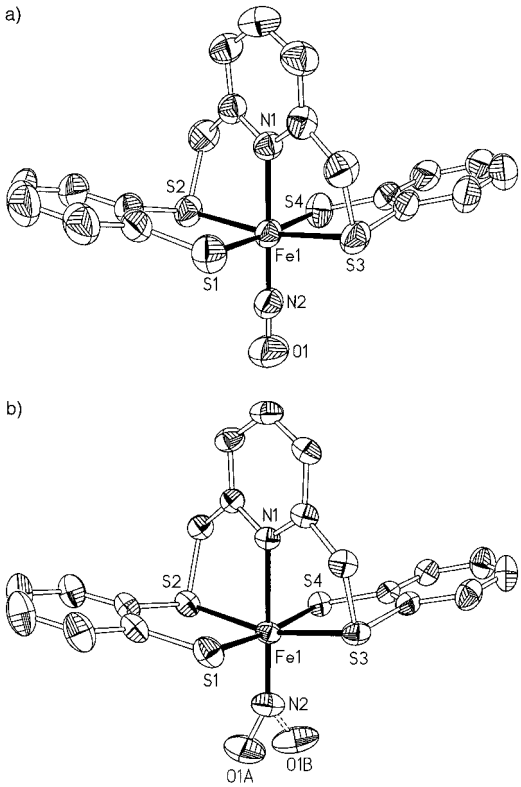

Figure 3. Molecular structures of a) the cation of [Fe(NO)($'pyS_4'$)]PF_6 ([**1**]PF_6); b) [Fe(NO)($'pyS_4'$)]·2CH_2Cl_2 (**2**·2CH_2Cl_2) (H atoms and solvate molecules omitted; the O atoms of the disordered NO ligand in **2**·2CH_2Cl_2 are indicated by O1A and O1B).

the molecular structures of the cation of [**1**]PF_6 and of neutral **2**. Table 1 lists selected distances and angles.

In both complexes, the Fe centers are pseudo-octrahedrally coordinated and exhibit identical connectivities such that the thiolate S donors adopt *trans* positions. The NO ligand in **2** is

Table 1. Selected distances [pm] and angles [°] of [Fe(NO)($'pyS_4'$)]PF_6 ([**1**]PF_6) and of [Fe(NO)($'pyS_4'$)]·2CH_2Cl_2 (**2**·2CH_2Cl_2).

	[**1**]PF_6	**2**·CH_2Cl_2		[**1**]PF_6	**2**·CH_2Cl_2
Fe1–N1	200.5(3)	216.7(2)	O1–N2–Fe1	179.5(3)	150.4(5)
Fe1–S1	231.3(2)	229.7(1)	O1B–N2–Fe1	–	143.8(5)
Fe1–S2	225.6(2)	230.1(1)	N1–Fe1–N2	178.8(2)	179.5(2)
Fe1–S3	225.4(2)	230.0(1)	S1–Fe1–S4	176.72(4)	172.90(3)
Fe1–S4	231.2(2)	229.7(1)	S2–Fe1–S3	168.58(4)	162.90(3)
Fe1–N2	163.4(3)	171.2(3)	S1–Fe1–S2	90.05(4)	89.34(3)
N2–O1	114.1(3)	115.8(6)	S1–Fe1–S3	89.93(4)	89.99(3)
N2–O1B	–	121.1(7)	N1–Fe1–S1	87.24(8)	86.11(6)
S1–C10	175.1(4)	175.0(3)	N1–Fe1–S2	84.67(8)	81.41(7)
S2–C15	177.7(4)	178.0(3)	N2–Fe1–S1	91.8(2)	93.4(1)
			N2–Fe1–S2	96.0(2)	98.4(1)

0947-6539/01/0709-1876 $ 17.50+.50/0 *Chem. Eur. J.* **2001**, *7*, No. 9

disordered. Two different orientations of the oxygen atom were refined, with an occupancy of 57 and 43%.

The comparison of $[\mathbf{1}]^+$ with **2** demonstrates that the unpaired electron in **2** causes significant effects in the Fe–N (pyridine), Fe–N (nitrosyl), Fe–S (thioether), and N–O distances. They all are elongated. Of the [Fe(NO)($'pyS_4'$)] core distances, only the Fe–S (thiolate) distances remain practically unchanged and they decrease very slightly from $[\mathbf{1}]^+$ to **2**. The Fe–N (pyridine) distance exhibits the most pronounced elongation and it increases by about 16 pm (216.7(2) versus 200.5(3) pm). This increase is followed by the approximately 8 pm increase of the Fe–N (nitrosyl) and the approximately 4.5 pm increase of the Fe–S (thioether) distances. Figuratively speaking, the addition of one electron to $[\mathbf{1}]^+$ inflates the $[FeN_2S_4]$ core into an ellipsoidal shape.

As a consequence thereof, relevant angles also change. In $[\mathbf{1}]^+$ and even more so in **2**, the Fe centers are located below the base plane of the square pyramid formed by the pyridine N and the four S atoms of the $'pyS_4'^{2-}$ ligand. This is indicated, for example, by the S1–Fe1–S4 and S2–Fe1–S3 angles. Whereas in $[\mathbf{1}]^+$ the angles are 176.72(4) and 168.58(4)°, in **2** the corresponding angles decrease to 172.90(3) and 162.90(3)°. The most important difference between $[\mathbf{1}]^+$ and **2** with regard to angles is the Fe–N–O angle. It is 179.5(3)° in $[\mathbf{1}]^+$, which indicates a practically linear FeNO entity, and it decreases to 150.4(5) and 143.8(5)° in **2**. The latter values are "halfway" between linear MNO and 120° MNO angles expected for complexes in which NO ligands with sp^2 hybridized N atoms bind to 16 VE metal complex fragments. Thus, the NO ligand in **2** can be anticipated to have experienced a considerable reduction from NO^+ (or NO) to NO^-. Such a reduction is possible only if the nineteenth electron occupies an antibonding π* (NO) orbital.

Density functional calculations: In order to determine the details of the electronic structure and, in particular, the nature of the bonding in $[\mathbf{1}]^+$ and **2**, we carried out density functional calculations on these compounds. We used the program TURBOMOLE[15] and employed the BP86 functional[16a, b] with a triple-zeta valence-polarized Gaussian basis set[17] for the structure determination, and the B3LYP functional[18] for the calculation of the Fe–NO binding energies in $[\mathbf{1}]^+$ and **2**.

The theoretical structure determination (geometry optimization) yielded bond lengths in good agreement with the X-ray structure determination (Table 2). However, in contrast to the X-ray structure determination, we found two inequivalent Fe–S (thioether) bond lengths of 226.4 and 236.3 pm for **2**; the bent FeNO moiety pointed in the direction of the shorter Fe–S bond (Figure 4a).

Table 2. Comparison of experimentally observed and calculated distances [pm] and FeNO angles [°] in $[\mathbf{1}]^+$ and **2**.

	$[\mathbf{1}]^+$ (theor.)	$[\mathbf{1}]^+$ (exp.)	**2** (theor.)	**2** (exp.)
Fe1–N1	204.5	200.5(3)	216.6	216.7(2)
Fe1–S1	233.8	231.3(2)	232.3	229.7(1)
Fe1–S2	228.2	225.6(2)	226.4	230.1(1)
Fe1–S3	228.3	225.4(2)	236.3	230.0(1)
Fe1–S4	233.4	231.2(2)	233.9	229.7(1)
Fe1–N2	164.0	163.4(3)	170.9	171.2(3)
N2–O1	115.0	114.1(3)	118.2	115.8(6)
O1–N2–Fe1	179.8	179.5(3)	149.0	150.4(5)

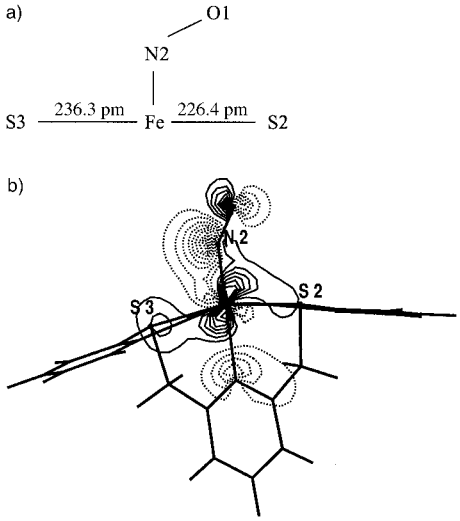

Figure 4. a) Short and long Fe–S (thioether) distances in the plane defined by the Fe, N, and thioether S atoms; b) Multicenter bonding and antibonding interactions in the [Fe(NO)(S2)(S3)] plane.

This inequivalence of the Fe–S (thioether) distances was not revealed by the X-ray structure analysis because the NO ligand is disordered so that only the average of the Fe–S (thioether) distances (230.0(1) pm) could be observed. The experimental average is very close to the theoretical average of 231.3 pm.

The different Fe–S (thioether) distances are plausibly explained by a bonding multicenter interaction between the Fe1, N2, and S2 atoms. This bonding interaction is supplemented by an antibonding interaction between N2 and S3 lobes on the opposite side (Figure 4b).

A calculation of the harmonic force field results in a frequency of 1698 cm^{-1} (exp. 1648 cm^{-1}) for the ν(NO) band in **2**, and 1923 cm^{-1} (exp. 1893 cm^{-1}) in $[\mathbf{1}]^+$. The differences in total energy of the complex fragment [Fe($'pyS_4'$)], $[\mathbf{1}]^+$, and **2** lead to Fe–NO bond energies of 455 kJ mol^{-1} and 91 kJ mol^{-1}, respectively. In agreement with the experimental findings we thus encounter a substantially weaker Fe–NO bond in the case of **2**.

The Kohn–Sham molecular orbitals were used for analyzing the electronic structure of our complexes. The S^2 value in the unrestricted Hartree–Fock wave function of **2** and also a limited multiconfiguration self-consistent field calculation in a smaller basis set do not indicate substantial multi-reference character for both compounds, which would render such an analysis questionable.

An analysis of the electronic structures of $[\mathbf{1}]^+$ and **2** by means of shared-electron numbers[19] shows that in **2** all bonds of Fe to its ligands are weakened due to antibonding interactions in the SOMO (Singly Occupied Molecular Orbital), which at the NO ligand has mainly π* orbital character, in agreement with qualitative MO theory.[20] Due to the lack of exact symmetry (and the inclination of the

Fe–NO bond with respect to the pseudo-tetragonal axis in **2**), the molecular orbitals are mixed heavily, and the picture is considerably more complex than in textbook examples. We found immediately below the HOMO (Highest Occupied Molecular Orbital) a quasiband of energetically closely spaced orbitals with strong metal–sulfur hybridization. The same holds true for the lowest unoccupied molecular orbitals, which are separated from the HOMO by a small energy gap.

In both complexes $[\mathbf{1}]^+$ and **2**, we can identify linear combinations of local σ and local π character at the NO, which describe bonding and antibonding interactions in line with qualitative theory. For example, in the case of $[\mathbf{1}]^+$, these interactions add up to a shared-electron number of 1.56 for the Fe–NO bond, which indicates almost a double bond; this number is diminished to 0.81 in **2**, which can be interpreted as a weak single bond. We find non-negligible multicenter character of most bonds at the iron center, and even two-center shared-electron numbers of about 0.04 for the interaction of the sulfur atoms with the nitrogen of NO, which also adds up to the observed bonding interaction. Moreover, substantial electron donation of the sulfur atoms to the iron center leads to a partial charge at the Fe atom. This charge is slightly negative in $[\mathbf{1}]^+$ when determined by means of three different methods of analysis (Mulliken population analysis, Roby–Davidson–Ahlrichs population analysis, and charge determination by means of Generalized Atomic Polar Tensors).[21]

Although these charges do not represent observables, they provide an explanation for the bonding differences in $[\mathbf{1}]^+$ and **2**. In $[\mathbf{1}]^+$ the $[FeL_x]$ metal ligand bonding is composed of covalent interactions enhanced by a substantial amount of ionic (Coulomb) interactions (semipolar bonds). In **2**, the ionic interactions are significantly reduced, and the remaining bonding is mainly covalent according to the following formula (formula B).

$$\underset{[\mathbf{1}]^+}{\overset{\delta-\quad\delta+}{Fe-L_X}} \longrightarrow \underset{\mathbf{2}}{\overset{0\quad 0}{Fe-L_X}}$$

Conclusion

The present work has shown that reactions of $[Fe(′pyS_4′)]_x$ or $[Fe(CO)(′pyS_4′)]$ with either $NOBF_4$ or NO gas yielded the corresponding 18 and 19 valence electron complexes $[Fe(NO)(′pyS_4′)]BF_4$ ($[\mathbf{1}]BF_4$) and $[Fe(NO)(′pyS_4′)]$ (**2**). Complexes $[\mathbf{1}]BF_4$ and **2** can be converted into each other by electrochemical or chemical redox reactions. Complex **2** is one of the rare 19 VE nitrosyl complexes which could be isolated and structurally characterized. Other structurally characterized 19 VE complexes are $[CpW(NO)_2PR_3]$,[22] [Fe(NO)(TPP)(4-methylpiperidine)],[23] and $[Fe(NO)(′N_HS_4′)]$,[7] but in these cases the structures of the 18 VE counterparts have remained unknown. The molecular structures of isolated 19 VE nitrosyl complexes such as $[Ru(NO)(py)_2Cl]I$,[24] $[Ru(NO)(py)_4Cl]PF_6$,[25] $[Fe(NO)(C_6H_4[As(Me)_2]_2)_2Cl]PF_6$,[26] and $[Fe(NO)(′tBuS_5′)]$[8, 14] have not been determined.

The X-ray structural characterization of $[\mathbf{1}]PF_6$ and **2** thus enabled us to compare directly and apparently for the first time the structural differences of strictly homologous 18 and 19 VE nitrosyl complexes. The metal donor distances of **2** versus $[\mathbf{1}]^+$ indicate that the unpaired electron of **2** populates a molecular orbital with metal donor antibonding character. DFT (Density Functional Theory) calculations supported the experimental findings and, in addition, revealed structural details such as different Fe–S (thioether) distances in **2**. The DFT calculations also confirm the antibonding character of the unpaired electron in **2**. In both $[\mathbf{1}]^+$ and **2**, the occupied orbitals close to the HOMO form a "valence band" of energetically closely spaced orbitals that provide flexibility for different binding modes of the FeNO moiety as well as the $[Fe(′pyS_4′)]$ core.

The antibonding character of the nineteenth electron rationalizes the high reactivity of **2**, which enables the rare NO/CO exchange reaction and the ready redox interconversion of $[\mathbf{1}]^+$ and **2**. The relatively high stability of **2**, on the other hand, could explain why so far no nucleophilic addition reactions with $[\mathbf{1}]^+$ have been achieved, in spite of its high frequency ν(NO) band.

Experimental Section

General remarks: Unless noted otherwise, all reactions and operations were carried out under nitrogen using standard Schlenk techniques. Solvents were dried and distilled before use. As far as possible, reactions were monitored by IR or NMR spectroscopy. Spectra were recorded on the following instruments: IR (KBr discs or CaF_2 cuvettes, solvent bands were compensated): Perkin Elmer 983, 1620 FT IR, and 16PC FT IR; NMR: Jeol-JNM-GX 270, EX 270, and Lambda LA 400 with the protio-solvent signal used as an internal reference. Spectra were recorded at 25 °C. Mass spectra: Jeol MSTATION 700 spectrometer; elemental analysis: Carlo Erba EA 1106 or 1108 analyzer; magnetic susceptibility: Johnson Matthey susceptibility balance; cyclic voltammograms: EG&G potentiostat PAR model 264A with glassy carbon working electrode, Pt counterelectrode, and Ag/AgCl reference electrode. Conducting electrolyte: NBu_4PF_6 (0.1M). Potentials were referred to NHE (Normal Hydrogen Electrode) with $Cp_2Fe^{0/+}$ as internal standard ($Cp_2Fe^{0/+} = 0.40$ V vs. NHE.[27]). Anhydrous hydrazine,[28] $[Fe(′pyS_4′)]_x$,[11] and $[Fe(CO)(′pyS_4′)]$[10] were prepared by literature methods. NEt_4N_3 was synthesized from NEt_4Cl and NaN_3 in MeOH and recrystallized from acetone.

$[Fe(NO)(′pyS_4′)]BF_4$ ($[\mathbf{1}]BF_4$)

a) *From* $[Fe(CO)(′pyS_4′)]\cdot MeOH$ *and* $NOBF_4$: At 0 °C, solid $NOBF_4$ (29 mg, 0.24 mmol) was added to a red solution of $[Fe(CO)(′pyS_4′)]\cdot$MeOH (115 mg, 0.24 mmol) in CH_2Cl_2 (15 mL). The green–brown reaction mixture was warmed up to room temperature within 5 h, stirred for another 10 h, and filtered. The filtrate was evaporated to give an oily residue. Extraction with CH_2Cl_2 (3 mL) and Et_2O (10 mL) afforded a brown powder, which was separated and washed with additional Et_2O (10 mL). The brown powder was redissolved in CH_2Cl_2 (12 mL) and Et_2O (4 mL) to give a green–brown solution. Upon cooling to −20 °C, a slight amount of brown solid precipitated and it did not exhibit a ν(NO) band. This solid was removed by filtration, and the green–brown filtrate was reduced in volume to 2 mL and combined with *n*-hexane (10 mL). A light brown solid precipitated, which was separated and dried in vacuo. Yield: 65 mg (49 %).

b) *From* $[Fe(′pyS_4′)]_x$ *and* $NOBF_4$: Under stirring, solid $NOBF_4$ (43 mg, 0.37 mmol) was added to a red–brown suspension of $[Fe(′pyS_4′)]_x$ (163 mg, 0.24 mmol) in CH_2Cl_2 (20 mL). After 24 h, the green–brown reaction mixture was filtered. The filtrate was reduced in volume to 1 mL and combined with THF (15 mL). The resultant light brown precipitate was separated and dried in vacuo. Yield: 155 mg (75 %).

^{1}H NMR (269.6 MHz, CD_2Cl_2): $\delta = 7.20–7.80$ (m, 10H; aryl), 7.63 (t, 1H; H_γ, pyridine), 5.56 (d, 2H; CH_2), 4.95 (d, 2H; CH_2); ^{13}C{^{1}H} NMR (100.4 MHz, CD_2Cl_2): $\delta = 156.3, 148.6, 137.9, 129.7, 129.4, 127.5, 126.0, 124.7,$

0947-6539/01/0709-1878 $ 17.50+.50/0 *Chem. Eur. J.* **2001**, *7*, No. 9

122.8 [C(aryl)], 51.6 [CH_2]; IR (KBr): $\tilde{\nu} = 1893\ cm^{-1}$ (NO), 1084 (BF_4); MS (FD, CH_2Cl_2): *m/z* (%): 471 [Fe(NO)('pyS_4')]$^+$; elemental analysis calcd (%) for $C_{19}H_{15}BF_4FeN_2OS_4$ (558.26): C 40.88, H 2.71, N 5.02, S 22.97; found C 41.06, H 2.77, N 4.88, S 22.81.

[Fe(NO)('pyS_4')] (2)

a) *From* [*Fe*('*pyS*$_4$')]$_x$ *and NO*: By means of a syringe, NO gas (6.4 mL, 0.26 mmol) was injected into a stirred red–brown suspension of [Fe('pyS_4')]$_x$ (115 mg, 0.26 mmol) in CH_2Cl_2 (20 mL). After 24 h, the resulting red–brown reaction mixture was filtered. The filtrate was reduced in volume to 1 mL and combined with Et_2O (30 mL). A brown solid precipitated, which was separated after 10 min and dried in vacuo. Yield: 90 mg (84 %).

b) *From* [*Fe*(*NO*)('*pyS*$_4$')]*BF*$_4$ *and* N_2H_4: Upon addition of N_2H_4 (11 μL, 0.38 mmol) to a stirred green–brown solution of [Fe(NO)('pyS_4')]BF_4 (105 mg, 0.19 mmol) in CH_2Cl_2 (20 mL) a deep red–brown solution resulted. After 20 min, it was reduced in volume to 1 mL. After addition of MeOH (20 mL), a brown powder precipitated, which was separated, washed with MeOH and *n*-hexane (10 mL each), and dried in vacuo. Yield: 65 mg (75 %).

^{1}H NMR (269.6 MHz, CD_2Cl_2): $\delta = 2.8$, 3.7, 4.2, 6.1, 23.0, 26.0; IR (KBr): $\tilde{\nu} = 1648\ cm^{-1}$ (NO); MS (FD, CH_2Cl_2): *m/z* (%): 471 [Fe(NO)('pyS_4')]$^+$; elemental analysis calcd (%) for $C_{19}H_{15}FeN_2OS_4$ (471.46): C 48.40, H 3.21, N 5.94, S 27.20; found C 48.24, H 3.35, N 5.70, S 27.03; $\mu_{eff} = 1.71$ B.M. (297 K).

[Fe(NO)('pyS_4')]PF_6 ([1]PF_6): At −78 °C, solid [Cp_2Fe]PF_6 (49 mg, 0.15 mmol) was added to a red–brown solution of [Fe(NO)('pyS_4')] (70 mg, 0.15 mmol) in CH_2Cl_2 (15 mL). The reaction mixture was kept at −78 °C for 20 min, subsequently warmed to room temperature, and filtered after 1 h. The green–brown filtrate was reduced in volume to 3 mL. Addition of Et_2O (10 mL) precipitated a brown powder, which was separated after 20 min, washed with Et_2O (20 mL), and dried in vacuo. Yield: 80 mg (88 %).

^{1}H NMR (269.6 MHz, CD_2Cl_2): $\delta = 7.20$–7.70 (m, 11 H; aryl, pyridine), 5.47 (d, 2 H; CH_2), 4.70 (d, 2 H; CH_2); ^{13}C{^{1}H} NMR (100.4 MHz, CD_2Cl_2): $\delta =$ 158.2, 150.8, 139.8, 131.6, 129.7, 127.9, 126.9, 124.7 [C(aryl, pyridine)], 55.8 [CH_2]; IR (KBr): $\tilde{\nu} = 1893\ cm^{-1}$ (NO), 836 (PF_6); MS (FD, CH_2Cl_2): *m/z* (%): 471 [Fe(NO)('pyS_4')]$^+$; elemental analysis calcd (%) for $C_{19}H_{15}PF_6FeN_2OS_4$ (661.42): C 37.02, H 2.45, N 4.54, S 20.81; found C 37.31, H 2.57, N 4.53, S 21.24.

[Fe(NO)$_2$('pyS_4')] (3)

a) *From* [*Fe*('*pyS*$_4$')]$_x$ *and NO*: By means of a syringe, NO gas (11.0 mL, 0.46 mmol) was injected into a stirred red–brown suspension of [Fe('pyS_4')]$_x$ (101 mg, 0.23 mmol) in CH_2Cl_2 (15 mL). After 3 h, an excess of NO gas (4 mL) was added, and the resulting red–brown reaction mixture was filtered after a total of 5.5 h. The filtrate was reduced in volume to 2 mL. After addition of Et_2O (20 mL), a brown powder precipitated, which was separated after 10 min, washed with Et_2O (5 mL), and dried in vacuo. Yield: 84 mg (73 %).

b) *From* [*Fe*(*CO*)('*pyS*$_4$')] · *MeOH and NO*: NO gas was bubbled through a red solution of [Fe(CO)('pyS_4')] · MeOH (80 mg, 0.16 mmol) in CH_2Cl_2 (30 mL) for 4.5 h. The resulting red–brown reaction mixture was stirred under an atmosphere of NO for an additional 12 h, filtered, and reduced in volume to 2 mL. After addition of Et_2O (20 mL), a brown powder precipitated, which was separated and dried in vacuo. Yield: 30 mg (38 %).

^{1}H NMR (269.6 MHz, CD_2Cl_2): $\delta = 7.00$–7.65 (m, 11 H; aryl, pyridine), 4.40 (m, 2 H; CH_2), 4.20 (m, 2 H; CH_2); IR (KBr): $\tilde{\nu} = 1812$ (sh), 1779, 1751 cm^{-1} (NO); MS (FD, CH_2Cl_2): *m/z* (%): 441 [Fe('pyS_4')]$^+$, 882 [Fe('pyS_4')]$_2^+$; elemental analysis calcd (%) for $C_{19}H_{15}FeN_3O_2S_4$ (501.46): C 45.51, H 3.01, N 8.38, S 25.58; found C 45.78, H 3.02, N 8.10, S 25.30.

X-ray structure analysis: At room temperature, dark brown single crystals of [**1**]PF_6 formed from a saturated solution in THF/Et_2O (7:1 by volume) over the course of three weeks. Brown single crystals of **2** · 2 CH_2Cl_2 were grown from a solution of **2** (70 mg) in CH_2Cl_2 (8 mL) at −20 °C over the course of four weeks.

Suitable single crystals of [**1**]PF_6 and **2** · CH_2Cl_2 were sealed under N_2 in glass capillaries without drying. Data were corrected for Lorentz and polarization effects. Absorption effects were corrected using Psi-scans for **2** · CH_2Cl_2, while for [**1**]PF_6 no correction was made (see Table 3). The structures were solved by direct methods (SHELXTL NT 5.1).[29] Full-matrix least-squares refinement was carried out on F^2 (SHELXTL NT 5.1). All non-hydrogen atoms were refined anisotropically. The anion in [**1**]PF_6 is disordered. Two different orientations were refined, which gave an occupancy of 59 % (F13A–F16A) and 41 % (F13B–F16B). In **2** · CH_2Cl_2, the NO ligand was disordered. Two different orientations were refined for the oxygen atom, with an occupancy of 57 % for O1A and 43 % for O1B. The compound crystallized with two molecules of CH_2Cl_2 per unit. Both solvent molecules were disordered. Two orientations for each CH_2Cl_2 molecule were refined. For the hydrogen atoms, only the main orientations were taken into account. The positions of all hydrogen atoms in [**1**]PF_6 and **2** · CH_2Cl_2 were taken from the difference Fourier map and refined with a common isotropic displacement parameter. Selected crystallographic data are summarized in Table 3.[30]

Table 3. Selected crystallographic data for [Fe(NO)('pyS_4')]PF_6 ([**1**]PF_6) and [Fe(NO)('pyS_4')] · 2 CH_2Cl_2 (**2** · 2 CH_2Cl_2).

	[**1**]PF_6	**2**
formula	$C_{19}H_{15}F_6FeN_2OPS_4$	$C_{21}H_{19}Cl_4FeN_2OS_4$
M_r [g mol^{-1}]	616.39	641.27
crystal size [mm]	0.60 × 0.40 × 0.30	0.60 × 0.50 × 0.38
F(000)	2480	650
crystal system	orthorhombic	triclinic
space group	*Pbca*	$P\bar{1}$
a [pm]	1466.9(4)	848.8(1)
b [pm]	1376.2(4)	1195.4(2)
c [pm]	2387.9(7)	1353.1(2)
α [°]	90	78.62(2)
β [°]	90	76.09(1)
γ [°]	90	85.32(2)
V [nm^3]	4.821(2)	1.3056(3)
Z	8	2
ρ_{calcd} [g cm^{-3}]	1.699	1.631
μ [mm^{-1}]	1.101	1.326
diffractometer	Nicolet R 3m/V	Siemens P4
radiation [pm]	$Mo_{K\alpha}$ ($\lambda = 71.073$)	$Mo_{K\alpha}$ ($\lambda = 71.073$)
temperature [K]	298	200
scan technique	ω-scan	ω-scan
2Θ range [°]	4.4–54.0	4.2–54.0
scan speed [° min^{-1}]	8	8
measured reflections	6395	6932
independent reflections	5266	5673
R_{int}	0.0303	0.0215
observed reflections	2765	4180
σ criterion	$F \geq 4.0\sigma(F)$	$F \geq 4.0\sigma(F)$
*R*1; *wR*2	0.0402; 0.0870	0.0386; 0.0915
refined parameters	389	394
abs. correction T_{min}/T_{max}	none	0.2392/0.3030

Acknowledgements

Support of this work by the Deutsche Forschungsgemeinschaft and the Fonds der Chemischen Industrie is gratefully acknowledged.

[1] a) V. Zang, R. van Eldik, *Inorg. Chem.* **1990**, *29*, 4462–4468; b) E. K. Pham, S. G. Chang, *Nature* **1994**, *369*, 139–141.

[2] a) S. Moncada, R. M. J. Palmer, E. A. Higgs, *Pharmacol. Rev.* **1991**, *43*, 109–142; b) M. Feelish, J. S. Stamler in *Methods in Nitric Oxide Research* (Eds.: M. Feelish, J. S. Stamler), Wiley, New York, **1996**, pp. 3–45; c) P. L. Feldman, O. W. Griffith, D. J. Stuehr, *Chem. Eng. News* **1993**, *71*, 26–31; d) A. R. Butler, D. L. H. Williams, *Chem. Soc. Rev.* **1993**, *22*, 223–241.

[3] T. Noguchi, J. Honda, T. Nagamune, H. Sasabe, Y. Inoue, I. Endo, *FEBS Lett.* **1995**, *358*, 9–12.

[4] M. W. J. Cleeter, J. M. Cooper, V. M. Darley-Usmar, S. Moncada, A. H. V. Scapira, *FEBS Lett.* **1994**, *345*, 50–54.

[5] a) J. B. Howard, D. C. Rees, *Chem. Rev.* **1996**, *96*, 2965–2982; b) B. K. Burgess, D. J. Lowe, *Chem. Rev.* **1996**, *96*, 2983–3012; c) R. R. Eady, *Chem. Rev.* **1996**, *96*, 3013–3030.

[6] a) F. Bottomley in *A Treatise on Dinitrogen Fixation* (Eds.: R. W. F. Hardy, F. Bottomley, R. C. Burns), Wiley, New York, **1979**, pp. 109–167; b) F. Bottomley, *Acc. Chem. Res.* **1978**, *11*, 158–163; c) J. A. McCleverty, *Chem. Rev.* **1979**, *79*, 53–76.
[7] D. Sellmann, H. Kunstmann, M. Moll, F. Knoch, *Inorg. Chim. Acta* **1988**, *154*, 157–167.
[8] D. Sellmann, K. Höhn, M. Moll, *Z. Naturforsch. B* **1991**, *46*, 665–672, and references therein.
[9] J. S. Yu, R. A. Jacobson, R. J. Angelici, *Inorg. Chem.* **1982**, *21*, 3106–3110.
[10] D. Sellmann, J. Utz, F. W. Heinemann, *Inorg. Chem.* **1999**, *38*, 5314–5322.
[11] D. Sellmann, N. Blum, F. W. Heinemann, unpublished results.
[12] D. Sellmann, K. Engl, F. W. Heinemann, *Eur. J. Inorg. Chem.* **2000**, *3*, 423–429.
[13] a) K. G. Caulton, *Coord. Chem. Rev.* **1975**, *14*, 317–355; b) M. Herberhold, A. Razavi, *Angew. Chem.* **1972**, *84*, 1150–1151; *Angew. Chem. Int. Ed. Engl.* **1972**, *11*, 1092–1093.
[14] D. Sellmann, K. Höhn, M. Moll, *Z. Naturforsch. B* **1991**, *46*, 673–681.
[15] R. Ahlrichs, M. Bär, M. Häser, H. Horn, C. Kölmel, *Chem. Phys. Lett.* **1989**, *162*, 165–169.
[16] a) A. D. Becke, *Phys. Rev. A* **1988**, *38*, 3098–3100; b) J. P. Perdew, *Phys. Rev. B* **1986**, *33*, 8822–8824.
[17] A. Schäfer, C. Huber, R. Ahlrichs, *J. Chem. Phys.* **1994**, *100*, 5829–5835.
[18] A. D. Becke, *J. Chem. Phys.* **1993**, *98*, 5648–5652.
[19] C. Ehrhardt, R. Ahlrichs, *Theor. Chim. Acta* **1985**, *68*, 231–245.
[20] T. A. Albright, J. K. Burdett, M.-H. Whangbo in *Orbital Interactions in Chemistry* (Eds.: T. A. Albright, J. K. Burdett, M.-H. Whangbo), Wiley, New York, **1985**.
[21] J. Cioslowski, *J. Am. Chem. Soc.* **1989**, *111*, 8333–8336.
[22] J. S. Yu, R. A. Jacobson, R. J. Angelici, *Inorg. Chem.* **1982**, *21*, 3106–3110.
[23] W. R. Scheidt, A. Ch. Brinegar, E. B. Ferro, J. F. Kirner, *J. Am. Chem. Soc.* **1977**, *99*, 7315–7322.
[24] K. Aoyagi, M. Mukaida, H. Kakihana, K. Shimuzu, *J. Chem. Soc. Dalton Trans.* **1985**, 1733–1734.
[25] R. W. Callahan, G. M. Brown, J. M. Meyer, *J. Am. Chem. Soc.* **1975**, *97*, 894–895.
[26] W. Silverthorn, R. D. Feltham, *Inorg. Chem.* **1967**, *6*, 1662–1666.
[27] H. M. Koepp, H. Wendt, H. Strehlow, *Z. Elektrochem.* **1960**, *64*, 483–491.
[28] H. Bock, *Z. Anorg. Allg. Chem.* **1958**, *293*, 264–273.
[29] *SHELXTL NT 5.1*, Bruker AXS, Madison, WI, **1998**.
[30] Crystallographic data (excluding structure factors) for the structures reported in this paper have been deposited with the Cambridge Crystallographic Data Centre as supplementary publication nos. CCDC-149005 ([**1**]PF_6) and CCDC-149006 (**2**$\cdot 2CH_2Cl_2$). Copies of the data can be obtained free of charge on application to CCDC, 12 Union Road, Cambridge CB2 1EZ, UK (fax: (+44) 1223-336-033; e-mail: deposit@ccdc.cam.ac.uk).

Received: October 10, 2000 [F2787]

  0947-6539/01/0709-1880 $ 17.50+.50/0